JOURNAL OF VIROLOGY, Mar. 1997, p. 2050–2058 Vol. 71, No. 3
0022-538X/97/$04.00+0

Position Dependence of Functional Hairpins Important for Human Immunodeficiency Virus Type 1 RNA Encapsidation In Vivo

M. SCOTT McBRIDE† AND ANTONITO T. PANGANIBAN*

McArdle Laboratory for Cancer Research, University of Wisconsin Medical School, Madison, Wisconsin 53706

Received 24 September 1996/Accepted 9 December 1996

At least two hairpins in the 5′ untranslated leader region, stem-loops 1 and 3 (SL1 and SL3), contribute to human immunodeficiency virus type 1 RNA encapsidation in vivo. We used a competitive assay, which measures the relative encapsidation efficiency of mutant viral RNA in the presence of competing wild-type RNA, to compare the contributions of SL1, SL3, and two adjacent secondary structures, SL2 and SL4, to encapsidation. SL2 is not required for RNA encapsidation, while SL1, SL3, and SL4 all contribute approximately equally to encapsidation. To determine whether these hairpins function in a position-dependent manner, we interchanged the positions of two of these stem-loop structures. This resulted in substantial diminution of encapsidation, indicating that the secondary structures that comprise E, the encapsidation signal, function only in their correct contexts. Mutation of nucleotides flanking SL1 and SL3 had little effect on encapsidation. We also showed that SL1, while present on both genomic and subgenomic viral RNAs, nonetheless contributes to selective encapsidation of genomic RNA. Taken together, these data are consistent with the formation of a higher-order RNA structure, partially composed of SL1, SL3, and SL4, that functions to effect concurrent encapsidation of full-length RNA and exclusion of subgenomic RNA. Finally, it has been reported that E is required for efficient translation of Gag mRNA in vivo. However, we have found that a variety of mutants, including a mutant lacking the entire region encompassing SL1, SL2, and SL3, still produce RNAs that are efficiently translated. These data indicate that E is unlikely to contribute to efficient Gag mRNA translation in vivo.

A *cis*-acting region that functions in human immunodeficiency virus type 1 (HIV-1) RNA encapsidation, referred to as either E or Ψ, is located downstream of the primer binding site extending to just within *gag* (1, 9, 15, 18, 21, 22, 25, 30). The in vitro secondary structure of this region appears to consist of four hairpins, based on biochemical probing and computer modeling (4, 10, 14). Previous results suggest that at least two of these hairpins, stem-loops 1 and 3 (SL1 and SL3), function as encapsidation elements in vivo (25). A double-hairpin structure has been shown to be required for encapsidation of other retroviral RNAs (19, 35). For spleen necrosis virus, encapsidation is reduced when the order of the two hairpins is reversed.

During encapsidation, genomic RNA is incorporated into the assembling virus particle while subgenomic RNA is largely excluded (22, 25). By locating a portion of the encapsidation signal downstream of the major subgenomic splice site (5′ss), HIV-1 is provided with a mechanism to specifically encapsidate genomic RNA. Spliced RNAs would not be encapsidated efficiently simply because they lack a portion of the E site. The selective encapsidation of genomic HIV-1 RNA involves sequences present within the viral intron, since mutations of SL3 result in disruption of selective encapsidation of genomic RNA (22, 25). However, other elements located upstream of the 5′ss that facilitate encapsidation, such as SL1, are present on both genomic and subgenomic HIV-1 RNAs. It is unclear whether such signals contribute to selective encapsidation of genomic RNA versus subgenomic RNA.

Internal ribosome entry sites (IRES) have been characterized for picornaviruses and for hepatitis C virus (16, 33). Murine leukemia virus (MuLV) appears to contain an IRES used for the translation of the nonglycosylated precursor $Pr65^{gag}$ (6, 34). The MuLV IRES is located just upstream of the $Pr65^{gag}$ start codon. The presence of an IRES in MuLV RNA has led some to ask whether the HIV-1 E, which is located at a position proximal to that of the HIV-1 *gag* gene, functions as an IRES (26). Preliminary data have suggested that E may be required for efficient translation of Gag mRNA in vivo but that it inhibits translation in vitro (26).

We carried out experiments to explore the contributions of individual hairpin structures to encapsidation and to see if these structures have the intrinsic ability to facilitate RNA packaging in vivo. Our data indicate that SL1, SL3, and SL4 contribute equivalently to encapsidation but that the function of SL1 and SL3 is position dependent. Since SL1 is an encapsidation element that is present on both full-length and spliced RNAs, we also carried out experiments to see if this structure contributes to discrimination between spliced and full-length RNAs during packaging. It appears that SL1 does play a role in selectivity, likely in conjunction with elements immediately downstream of the splice donor. We also examined the translational expression of Gag mRNA in mutants lacking the E region. It appears that E is not required for efficient translation of Gag mRNA.

MATERIALS AND METHODS

Construction of plasmid DNAs. Standard techniques were used for molecular cloning (23). The creation of pMSMBA, pS1, pS2, pS3, pS4, pS1/S1′S3, and

* Corresponding author. Mailing address: McArdle Laboratory for Cancer Research, University of Wisconsin Medical School, 1400 University Ave., Madison, WI 53706. Phone: (608) 263-7820. Fax: (608) 262-2824. E-mail: Panganiban@oncology.wisc.edu.

† Present address: Department of Molecular Microbiology, Washington University School of Medicine, St. Louis, MO 63110-1093.

pS1S3′/S3 has been described previously (25). pS1/S1′ was created by the same strategy as pS1/S1′S3, with pMSMBA being used as a template for PCR mutagenesis as previously described (25). pS3′/S3 was created by cloning the *Bsp*EI-to-*Bss*HII fragment of pMSMBA into pS1S3′/S3. pdM was created by ligation of two fragments obtained by PCR amplification of pMSMBA with two sets of primers, the sense primer 275–298 (25) with the antisense mismatch primer 707–684 *Mlu*I (5′-AGCAAGCCGACGCGTGCGTCGAGA) and the sense mismatch primer 721–744 *Mlu*I (5′-CAAGAGGCGACGCGTGGCGACTGG) with the antisense primer 1535–1511 (25). The two fragments were digested with *Mlu*I and ligated. The ligation mixture was then amplified with the sense primer 275–298 and the antisense primer 1535–1511 to generate a 1,223-bp fragment containing a 37-nucleotide (nt) deletion from nt 696 to 732 and point mutations at nt 694, 733, and 735. The fragment was digested with *Bsp*EI and *Spe*I and ligated to pMSMBA which had been digested with *Bsp*EI and *Spe*I. pdX was generated in a fashion similar to pdM, with the two mismatch primers 774–751 *Xba*I (5′-CTCCGCTAGTCTAGATTTTTGGCG) and 772–795 *Xba*I (5′-GAG GCTAGATCTAGAGAGATGGGT) being used. pdX contains a 21-nt deletion from nt 763 to 783 and a point mutation at nt 761. pdMX was created in a fashion similar to pdM, with pdX being used as the template for PCR amplification in place of pMSMBA. pSL3SL1 was created in two steps. First, a fragment was generated by PCR amplification of pdMX with the primers 275–298 and M693+SL3 (5′-GCAGCGCGCTCTAGCCTCCGCTAGTGCGTCGAGAGAT CTCCTCTG). This fragment was digested with *Bsp*EI and *Bss*HII and ligated into pdMX which had been digested with *Bsp*EI and *Mlu*I, creating pSL3dX. Next, a fragment was generated by PCR amplification of pSL3dX with primers 275–298 and X760+SL1 (5′-CGCACTAGTCCTCGCCTCTTGCCGTGCGCG CTTCAGCAAGCCGAGAGATTTTTGGCGTACTCA). This fragment was digested with *Bsp*EI and *Spe*I and ligated into pSL3dX which had been digested with *Bsp*EI and *Xba*I, generating pSL3SL1. pSL1SL3 was created in two steps. First, a set of overlapping oligonucleotides, S1(+) (5′-CGCGTCTCGCCTCTT GCCGTGCGCGCTTCAGCAAGCCGCGT) and S1(−) (5′-CGCGACTCGG CTTGCTGAAGCGCGCACGGCAAGAGGCGAGA), was ligated into pdMX which had been digested with *Mlu*I, creating pSL1dX. Next, another set of overlapping oligonucleotides, S3(+) (5′-CTAGACTAGCGGAGGCTAGAG GA) and S3(−) (5′-CTAGTCCTCTAGCCTCCGCTAGT), was ligated into pMSL1 which had been digested with *Xba*I, to creating pSL1SL3. pdM-X was created by digesting pdMX with *Mlu*I and *Xba*I, treating the DNA with Klenow enzyme (23), and ligating the larger fragment. pdGPE was created by digesting pMSMBA with *Pst*I and ligating the larger fragment. p5′ssβglob was created by ligating the overlapping oligonucleotides 5′ssβglob(+) (5′-CGCGTTGCGGCC CTGGGCAGGTTGGTATCAAGGTTT) and 5′ssbglob(−) (5′-CTAGAAACC TTGATACCAACCTGCCCAGGGCCTCAA) into pdMX which had been digested with *Mlu*I and *Xba*I. The creation of pGEM(600–900) has been described previously (25). pGEM(600–1000) was created by PCR amplification of pMSMBA with the primer pair 587–610 *Bam*HI (25) and 1010–987 *Xho*I (5′-T CTTCTGATCTCGAGTGAAGGGAT). The resulting 423-nt fragment was digested with *Bam*HI and *Xho*I and ligated into pGEM11zf(−) digested with the same two enzymes.

Transfections. Twenty-four hours before transfection, 293 cells were seeded at a density of 10^7 per 150-mm-diameter plate in 30 ml of Dulbecco's modified Eagle medium supplemented with 10% fetal bovine serum and incubated at 37°C in 5% COi2. Transfections were carried out with 30 mg of each plasmid DNA per 150-mm-diameter plate by the calcium phosphate precipitation method as previously described (25). Cotransfections were performed with 15 mg of each of the two plasmids being transfected, for a total of 30 mg of DNA.

RNA isolation from cytoplasm and virions. After 48 to 72 h, the medium and cytoplasmic RNA were concurrently collected. The cytoplasmic RNA was harvested as previously described (23), and the concentration was determined by measuring the spectrophotometric absorption at 260 nm. Virus was harvested from the medium by first removing cellular debris by centrifugation at 4,000 rpm in a Beckman AccuspinFR tabletop centrifuge. The virus was then pelleted from the clarified medium by centrifugation through a 20% sucrose cushion for 2.5 h at 25,000 rpm in an SW28 rotor. The viral pellet was resuspended in TNE buffer (10 mM Tris-HCl [pH 7.4], 100 mM NaCl, 1 mM EDTA). The physical virus titer was determined by using an antigen-capture assay to quantitate p24 (Coulter Cytometry). To isolate RNA from virions, the latter were disrupted by the addition of sodium dodecyl sulfate to 1% and incubation in a boiling water bath for 5 min. The sample was then treated with proteinase K (500 mg/ml) at 37°C for 30 min followed by phenol (pH 4.5)-chloroform extraction, chloroform extraction, and ethanol precipitation in the presence of 20 mg of poly(C) RNA. Both the nucleic acid isolated from the cytoplasm of the transfected cells and that isolated from the virus were treated with DNase I by resuspending the isolated nucleic acid in 50 ml of a buffer containing 10 mM Tris-HCl (pH 7.4), 10 mM $MgCl_2$, 40 U of RNasin (Promega), 1 mM dithiothreitol, and 10 U of RNase-free DNase I (Boehringer Mannheim). The nucleic acid was incubated at 37°C for 30 min. To terminate the reaction, the samples were treated with proteinase K, phenol-chloroform extracted, chloroform extracted, and precipitated with ethanol.

RNase protection. The antisense probe ($\sim 10^8$ cpm/mg) was synthesized by transcription of pGEM(600–900) or pGEM(600–1000) with T7 RNA polymerase (Promega) following linearization with *Not*I by a described protocol (23). To serve as size markers for denaturing polyacrylamide gels, ^{32}P-end-labeled fragments of pGEM11zf(−) digested with *Hpa*II were synthesized (23). Either 25 mg of cytoplasmic RNA or one-fifth of the virion RNA preparation supplemented with 25 mg of poly(C) RNA was mixed with 10^6 Cerenkov counts of ^{32}P-labeled antisense RNA (~6 fmol) and precipitated with ethanol. Samples were washed with 70% ethanol and resuspended in 20 ml of hybridization buffer (100 mM sodium citrate [pH 6.4], 300 mM sodium acetate [pH 6.4], 1 mM EDTA in 80% formamide), heated at 95°C for 3 min, and hybridized at 42°C for 16 h. Two hundred milliliters of RNase digestion mixture (10 mM Tris-HCl [pH 7.4], 300 mM NaCl, 5 mM EDTA, 2 mg of RNase T_1 per ml, 5 mg of RNase A per ml) was added for a 30-min incubation at 37°C. Sodium dodecyl sulfate was added to 1%, and proteinase K was added to 0.5 mg/ml. Samples were incubated for 30 min at 37°C, phenol-chloroform extracted, chloroform extracted, and precipitated with ethanol in the presence of 25 mg of poly(C) RNA carrier. Pellets were dissolved in 10 ml of formamide loading buffer (2 mM EDTA [pH 8.0] in 80% formamide), heated at 95°C for 3 min, and subjected to polyacrylamide gel electrophoresis (6% polyacrylamide [19:1 acrylamide-bisacrylamide], 8 M urea). Quantitation of the various protected RNA species was achieved by PhosphorImager analysis (Molecular Dynamics).

RESULTS

Relative contributions of SL1, SL2, SL3, and SL4 to encapsidation. SL1 and SL3 were previously shown to be important in encapsidation in both competitive and noncompetitive assays (25). Competitive assays measure the relative encapsidation efficiencies of coexpressed wild-type and mutant RNAs in virus-producing cells (22). Noncompetitive assays measure encapsidation efficiency by quantitating encapsidation for wild-type and mutant RNAs expressed separately from different virus-producing cell populations. In addition to SL1 and SL3, the E region contains a hairpin, SL2, which spans the major subgenomic splice donor and is located between SL1 and SL3. A fourth hairpin, SL4, is located just within the *gag* gene. We used a competitive assay to compare the relative contribution of each of these structures to encapsidation. First, 293 cells were cotransfected with both pMSMBA (wild type) and a plasmid containing point mutations that affect the stability of the predicted secondary structure of the encapsidation signal (Fig. 1A). The cytoplasmic RNA was isolated from these cells, and the virion RNA was isolated from the medium as previously described (25); both were subjected to RNase protection analysis with a riboprobe capable of detecting both wild-type and mutant RNAs (Fig. 1B). The relative encapsidation efficiencies of the mutants were determined by calculating the ratio of mutant RNA to wild-type RNA in the virion relative to the ratio of the two RNAs in the cytoplasm (Table 1). The results of this experiment indicate that mutations in SL2 have only a slight effect on the relative encapsidation efficiency of genomic RNA (compare 0.80 with 1.0 for the wild type) while mutations in SL4 have a larger effect (0.44). Mutations in SL1 (0.39) and SL3 (0.31) also reduce the relative encapsidation efficiency of genomic RNA, and second site mutations designed to restore base pairing within the stems restore encapsidation efficiency (0.83 and 0.82, respectively).

The function of SL1 and SL3 is dependent on the relative order of these hairpins within the encapsidation signal. Hairpin structures such as SL1, SL3, and SL4 may individually contribute to encapsidation. Alternatively, these secondary structures may function only in their proper context in a manner indicative of a more highly ordered region where exact displaying of SL1, SL3, and SL4 is required for recognition during encapsidation. Thus, we attempted to determine whether a pair of intact hairpin structures can function when their positions are reversed. We constructed pdM, in which SL1 is precisely deleted and an *Mlu*I site is created in its place, and pdX, in which SL3 is precisely deleted and an *Xba*I site is created in its place. pdMX contains both deletions (Fig. 2A). We also generated a mutant, pSL3SL1, in which SL1 and SL3 were inserted into pdMX in the reverse positions (Fig. 2B).

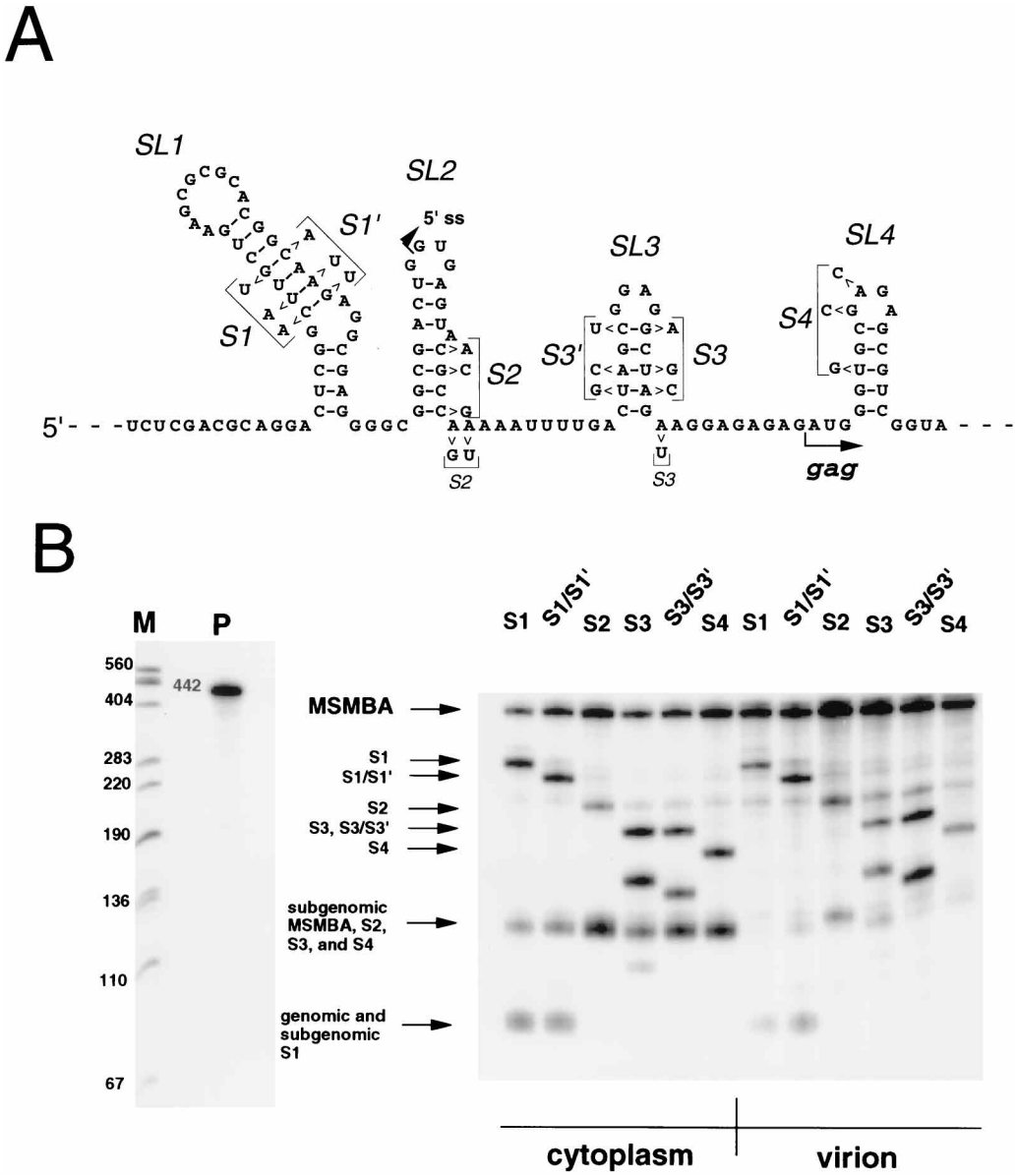

FIG. 1. Relative contributions of SL1, SL3, and SL4 to encapsidation. (A) Secondary structure of HIV-1 RNA nt 230 to 356 and groups of mutations within SL1, SL2, SL3, and SL4. The nomenclature is the same as that used by Clever et al. (10). The mutants S1/S1′ and S3/S3′ are double mutants containing both primary mutations and second site mutations. (B) Representative RNase protection analysis. Each of the plasmids was cotransfected with pMSMBA, and RNA was isolated from both cytoplasm and virions and subjected to RNase protection analysis. The marker (M; in nucleotides) was generated as described previously (25). The antisense probe (P) was generated from pGEM(600–1000), which contains a pMSMBA DNA fragment from nt 601 to 996 inserted into the *Bam*HI and *Xho*I sites of pGEM11zf(−) (Promega). The antisense riboprobe was generated by linearizing pGEM600–1000 with *Not*I and transcribing with T7 polymerase in the presence of [^{32}P]CTP. The riboprobe contains pMSMBA RNA nt 542 to 147. The amount of probe loaded on the gel is 1/40 the amount used in RNase protection. The diagnostic bands for genomic MSMBA (wild type), S1, S1/S1′, S2, S3, S3/S3′, and S4 RNAs are 395, 291, 272, 245, 216, 216, and 197 nt in length, respectively. The 142-nt band represents subgenomic MSMBA, S2, S3, S3/S3′, and S4 RNA. The 101-nt band represents genomic and subgenomic S1 and S1/S1′ RNA.

Finally, we constructed a control mutant, pSL1SL3, in which SL1 and SL3 were reinserted into pdMX at the *Mlu*I and *Xba*I sites, respectively (Fig. 2C). This mutant contains all four hairpins in the same relative positions as in wild-type RNA but also contains the same mutations that flank the inverted hairpins in pSL3SL1. Since these flanking point mutations all fall within the spacer regions between discrete hairpin structures, this mutant is also potentially useful for assessing the importance of these nucleotides in encapsidation. The relative encapsidation efficiencies of RNA expressed from each of these plasmids were then determined (Fig. 3; Table 1). The encapsidation efficiency of pSL1SL3 was only slightly reduced (0.82). This indicates that the mutations flanking the hairpin structures have little effect on encapsidation. In contrast, pdM, pdX, and pdMX all exhibited reduced encapsidation efficiencies (0.15, 0.20, and 0.10, respectively). The reductions in relative encapsidation of these RNAs were consistent with those observed for RNAs containing mutations that ablate stable stem formation. Moreover, pSL3SL1 had a reduced relative encapsidation efficiency (0.24). This indicates that the order of SL1 and SL3 cannot be reversed without affecting encapsidation. Examination by Mfold of both optimal and suboptimal stable secondary

TABLE 1. Relative encapsidation efficiencies of RNAs containing mutations in E

Mutant[a]	Relative encapsidation efficiency[b]
S1	0.39 ± 0.11
S1/S1′	0.83 ± 0.19
S2	0.80 ± 0.08
S3	0.31 ± 0.14
S3/S3′	0.82 ± 0.12
S4	0.42 ± 0.09
dM	0.20 ± 0.05
dX	0.15 ± 0.03
dMX	0.10 ± 0.03
SL3SL1	0.24 ± 0.07
SL1SL3	0.82 ± 0.13

[a] All mutants are derivatives of pMSMBA.

[b] The relative encapsidation efficiency of each mutant was calculated by dividing the ratio of mutant RNA to MSMBA RNA in the virion by the ratio of mutant RNA to MSMBA RNA in the cytoplasm as determined by RNase protection analysis (see legends to Fig. 1B and 3). The results represent means ± standard deviations from at least three independent experiments.

structures formed in pSL3SL1 RNA indicated that SL1, SL2, SL3, and SL4 would all be expected to form (data not shown). Overall, these data are consistent with the presence of a higher-order structure in HIV-1 RNA containing SL1, SL3, and SL4 and a requirement for correct, position-dependent displaying of those hairpins.

Mutations in SL1 cause a relative increase in encapsidation of spliced viral RNA. Encapsidation elements located distal to the splice donor, such as SL3 and SL4, are present only in genomic RNA since they are removed by splicing from subgenomic RNA. Hypothetically, the presence of SL3 and SL4 in full-length RNA would be sufficient to allow incorporation of genomic RNA into the assembling virus particle while spliced RNA would be excluded. Consistent with this hypothesis, Luban and Goff (22) showed that mutations causing ablation of SL3 resulted in decreased discrimination between genomic and subgenomic RNAs. However, in some of our experiments, we noticed that mutation of SL1 also appeared to reduce discrimination. To investigate this possibility more carefully, we transfected 293 cells with pMSMBA or pS1. RNA isolated from the cytoplasm of the transfected cells and RNA isolated from equivalent physical titers (equal p24 units) of virion particles were subjected to RNase protection analysis (Fig. 4A). The total amount of genomic and subgenomic viral RNA per virion for the S1 mutant was only slightly reduced relative to that observed for MSMBA (0.74 and 1.07, respectively) (Fig. 4B). However, although the encapsidation efficiency of S1 genomic RNA was reduced to about half that of the wild type, there was a concurrent increase in the encapsidation of S1 subgenomic RNA (Fig. 4B). These data suggest that the presence of SL1 in genomic RNA contributes to the selective encapsidation of genomic RNA and to the exclusion of subgenomic RNA from virus particles. This is consistent with the idea that SL1, SL3, and SL4 together comprise an efficiently recognized higher-order RNA structure. Disruption of part of that signal, even a component proximal to the 5′ss, reduces the ability of the virus to discriminate between genomic and subgenomic RNA.

Gag is expressed efficiently in the absence of SL1, SL2, and SL3. Genomic RNA is indistinguishable from Gag mRNA. By studying a large set of mutations in E, we previously found that Gag expression in vivo was efficient in the absence of E provided that the 5′ss was maintained (25). These data were seemingly at odds with a recent report which suggested that an intact E region was required for efficient expression of Gag in vivo (26). To analyze the importance of the HIV-1 E in translation more systematically, we assessed the ability of pdMX and derivatives of pdMX to express Gag as determined by a p24 antigen capture assay (Coulter Cytometry). We first created a derivative of pdMX called pdM-X in which the entire sequence in between the *Mlu*I and *Xba*I sites containing the 5′ss and SL2 is deleted (Fig. 5A). Since pdM-X lacks a 5′ss, expression of subgenomic mRNAs should be deficient in this mutant. Thus, a transcomplementing plasmid called pdGPE (Fig. 5B), which is a derivative of pMSMBA containing a *Pst*I-*Pst*I deletion of DNA nt 1409 to 2843 within *gag* and *pol*, was used to provide Tat and Rev in *trans*. pdGPE, which encodes a Gag protein that lacks a significant portion of the capsid domain, does not express p24. In addition, we analyzed Gag expression from a plasmid designated p5′ssβglob (Fig. 5C), which contains the 5′ss from the first intron of the β-globin gene inserted in between the *Mlu*I and *Xba*I sites in pdMX. The intracellular viral RNA level of each of these mutants was determined by transfecting 293 cells with pMSMBA or a mutant plasmid in parallel, preparing cytoplasmic extracts, and performing an RNase protection assay as described in the legend to Fig. 4. For each transfection, the amount of intracellular genomic RNA was determined and compared to that of pMSMBA (Fig. 6A and B). All of the mutants produced smaller amounts of steady-state genomic RNA (Gag mRNA) than the wild type with the exception of pdGPE, which expressed similar amounts. Additionally, the ratios of genomic to subgenomic viral RNA were determined for each transfection and found to be similar, indicating that the mutations do not affect splicing (data not shown).

To examine translation efficiency, the intracellular concentration of p24 in the cytoplasm was determined by a p24 antigen capture assay. All of the mutants, including p5′ssβglob, expressed readily detectable levels of cytoplasmic p24 except pdM-X and pdGPE, which expressed p24 at low and background levels, respectively (Fig. 6B). However, when pdM-X and pdGPE were transfected into cells together, p24 expression was increased markedly. To assess overall translation efficiency, ratios of cytoplasmic p24 RNA to genomic RNA were calculated for each transfection and normalized to that of pMSMBA. All of the mutants that expressed detectable p24 had ratios of cytoplasmic p24 to genomic RNA that were higher than that of the wild type, indicating that the E is not required for translation in vivo. In fact, provided that the cytoplasmic RNA is not in excess for translation, pdMX and p5′ssβglob mRNAs appeared to be translated more efficiently than wild-type RNA.

To verify that these mutants were defective in encapsidation as expected, RNA was extracted from equivalent p24 units in the medium and subjected to RNase protection analysis (Fig. 6A). Since the 293 cells transfected with pdM-X in the absence of pdGPE expressed such a small amount of p24, virions produced from this transfection were excluded from this analysis. The results of this experiment show that genomic RNAs from pdMX and p5′ssβglob are defective in their ability to be encapsidated (Fig. 6C). Additionally, only a small amount of pdM-X RNA (relative encapsidation efficiency, 0.02) was detected in the virions produced by cotransfection of pdM-X and pdGPE, demonstrating that pdM-X is defective in encapsidation. Interestingly, genomic RNA from pdGPE is encapsidated as well as that of the wild type, indicating that the deletion within pdGPE does not remove *cis* elements essential for RNA encapsidation. Finally, genomic RNA expressed from p5′ssβglob was inefficiently encapsidated (relative encapsidation efficiency, 0.08).

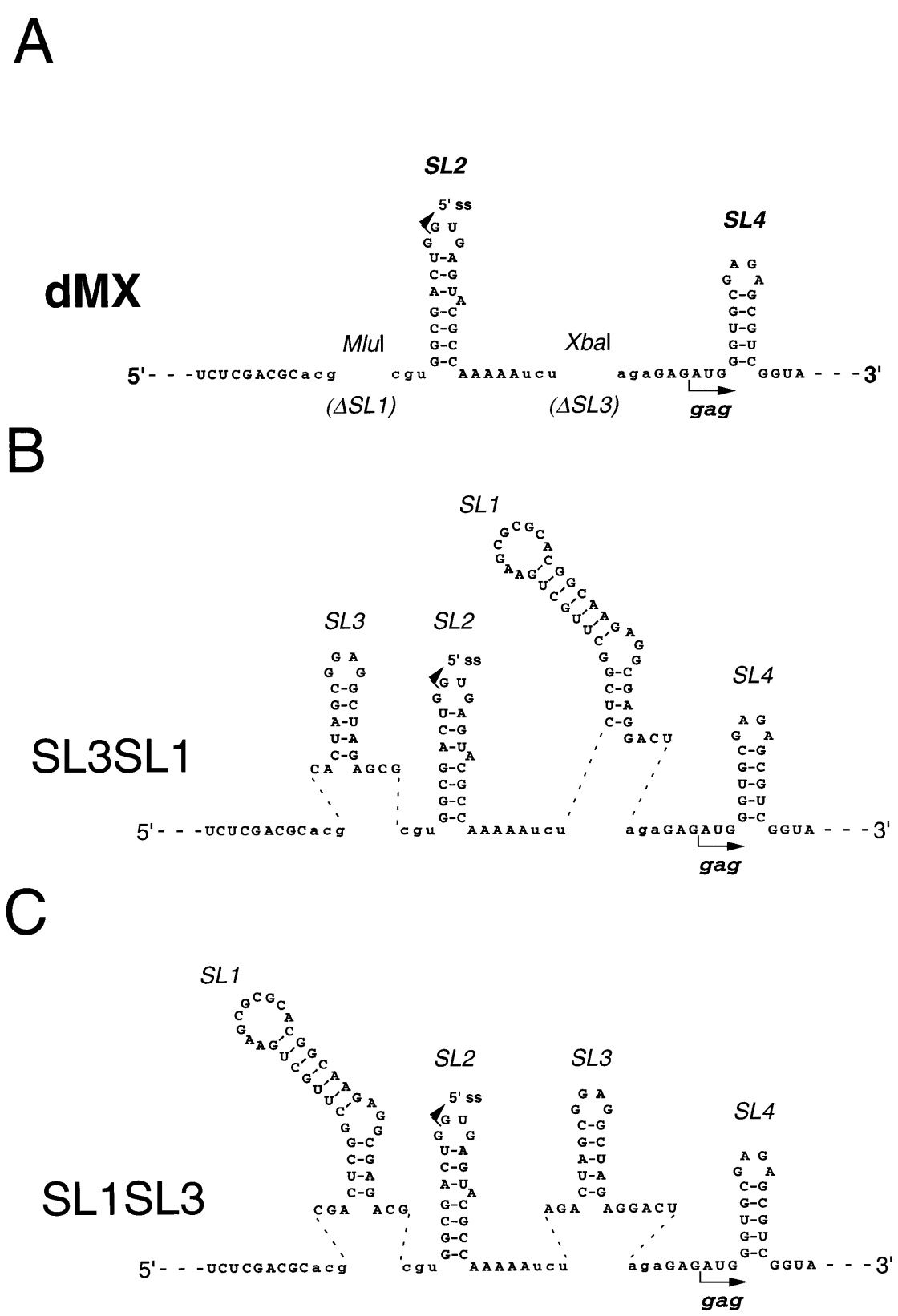

FIG. 2. Plasmids used to study the effect of the positions of SL1 and SL3 on encapsidation. (A) In pdM, SL1 has been precisely deleted and an *Mlu*I site has been introduced. For pdX, SL3 has been precisely deleted and an *Xba*I site has been inserted. Mutations introduced in the regions flanking SL1 and SL3 are indicated by lowercase letters. For pdMX, SL1 and SL3 have been precisely deleted *Mlu*I and *Xba*I sites, respectively, have been inserted. (B) For pSL3SL1, SL3 and SL1 have been inserted into the *Mlu*I and *Xba*I sites of pdMX. (C) For pSL1SL3, SL1 and SL3 have been inserted into the *Mlu*I and *Xba*I sites, respectively, of pdMX.

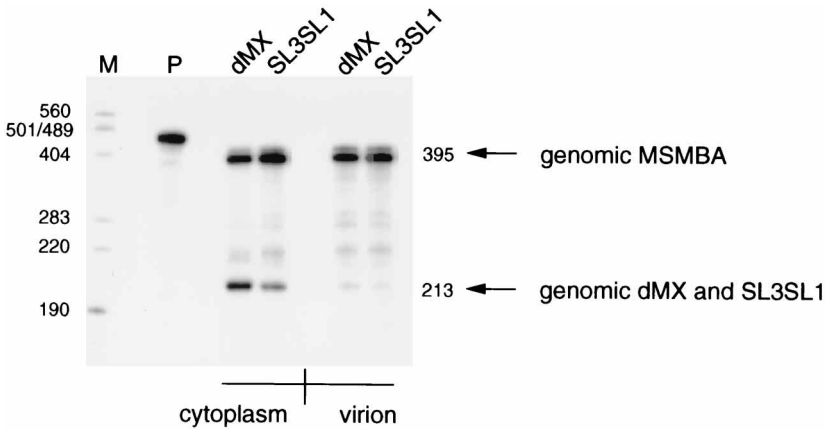

FIG. 3. The function of SL1 and SL3 in encapsidation is position dependent. (A) Representative RNase protection analysis of dMX and SL3SL1. 293 cells were cotransfected with pMSMBA and either pdMX or pSL3SL1, and RNase protection analysis was performed on cytoplasmic RNA and virion RNA as described in the legend to Fig. 1.

DISCUSSION

We have analyzed the secondary structure of the E of HIV-1 RNA. Although additional regions of the genome appear to play a role in encapsidation (8, 17, 22, 25, 30, 31), our study focused on the region downstream of the primer binding site extending into *gag*. Two stem-loops within this region, SL1 and SL3, are clearly important in encapsidation. Mutations that affect putative hairpin SL4 also reduce encapsidation efficiency

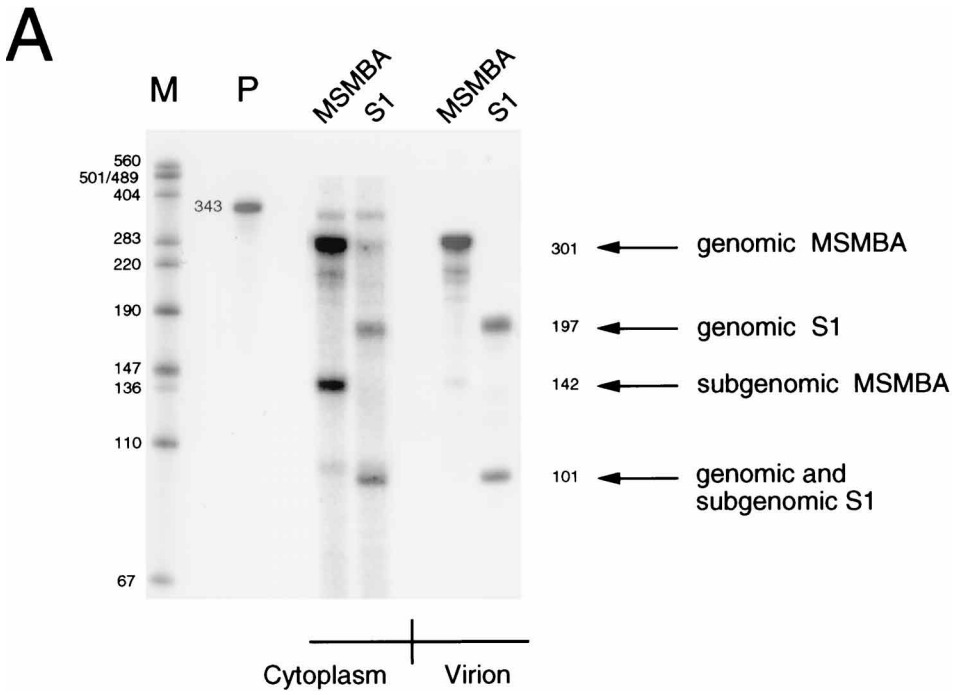

B

	Cytoplasm			Virion		
	genomic	subgenomic	total	genomic	subgenomic	total
MSMBA	1.00	0.72	1.72	1.00	0.07	1.07
S1	0.23	0.33	0.56	0.50	0.24	0.74

FIG. 4. SL1 contributes to selective encapsidation of genomic RNA relative to subgenomic RNA. (A) RNase protection analysis. 293 cells were transfected with either pMSMBA or pS1 in parallel, and RNase protection was performed with a riboprobe generated from pGEM(600–900) linearized at the *Not*I site and transcribed with T7 RNA polymerase in the presence of [^{32}P]CTP. Analysis was performed on RNA isolated from equivalent amounts of cytoplasm or RNA isolated from equivalent amounts of virions as determined by a p24 antigen capture assay (Coulter Cytometry). See the legend to Fig. 1 for explanations of M and P. (B) The molar amounts of viral RNAs were determined relative to genomic MSMBA RNA (1.00). The amount of subgenomic S1 RNA was determined by subtracting the amount of genomic S1 RNA (197-nt band) from the total S1 RNA (101-nt band).

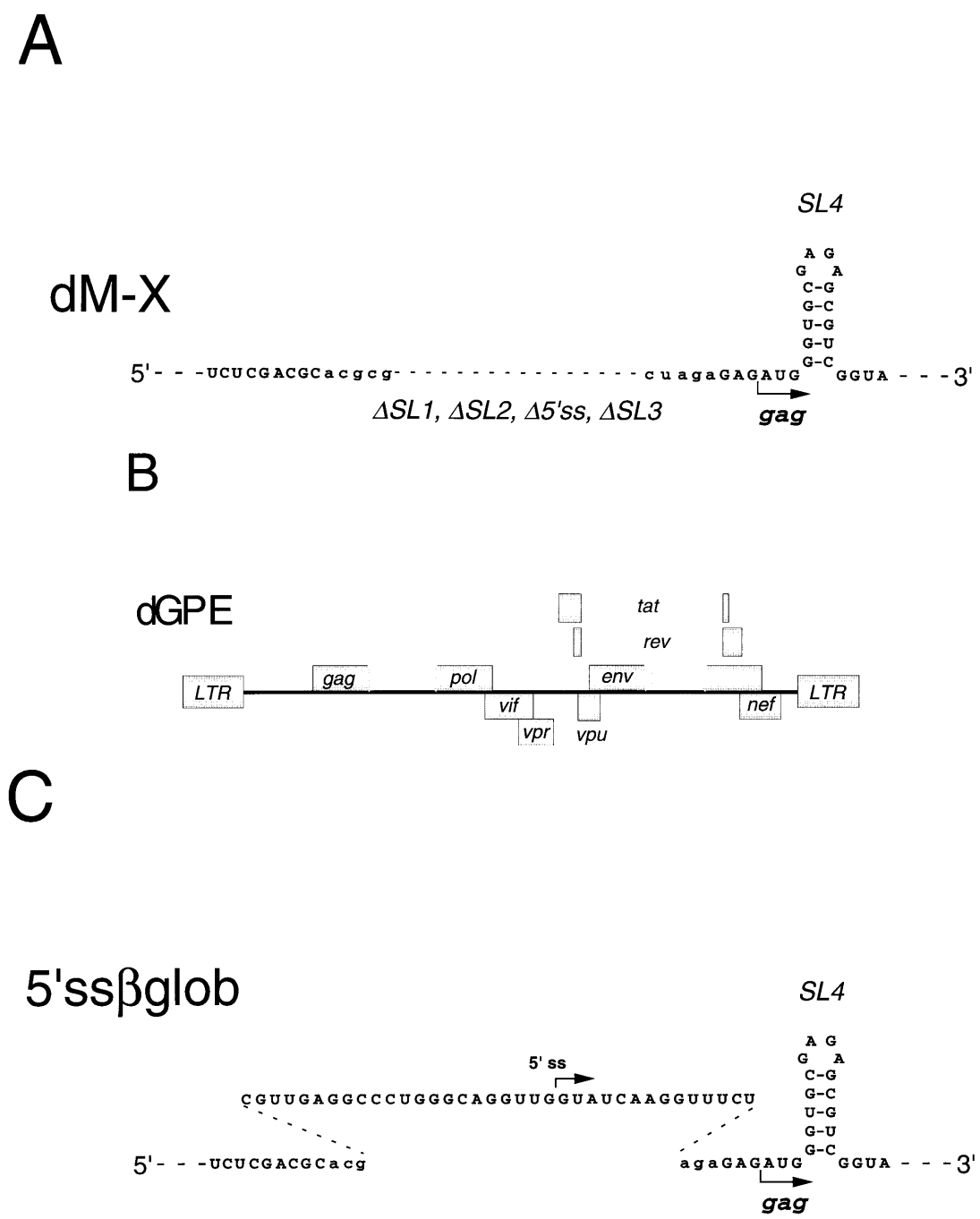

FIG. 5. Plasmids used to study translation in the absence of E. (A) pdM-X contains a deletion between the *Mlu*I and *Xba*I sites of pdMX. (B) pdGPE is a derivative of pMSMBA with a deletion between the *Pst*I sites that lie within *gag* and *pol*. LTR, long terminal repeat. (C) p5′ssβglob contains an insertion of a portion of the sequence spanning the 5′ss of the first intron of the β-globin gene in between the *Mlu*I and *Xba*I sites of pdMX.

to an extent similar to that observed by others (22) and to a magnitude similar to that of mutations in SL1 and SL3. SL2 does not appear to be a functional secondary structure in encapsidation since base substitutions within SL2 have little effect on encapsidation efficiency. Two alternative stem-loops have been suggested for SL2 (10, 14), and our pS2 group of mutations would disrupt base pairing within the stems of both of these alternative secondary structures.

The fact that the positions of SL1 and SL3 cannot be reversed without diminishing encapsidation suggests that the hairpin structures that are required for encapsidation are situated within a higher-order structure and that their function requires exact presentation of individual components of that structure. It is attractive to visualize a model in which SL1, SL3, and SL4 are precisely displayed and act in concert with one another to form an optimal higher-order structure that is recognized during packaging. Clever et al. (10) have shown that SL1, SL3, and SL4 are binding sites for Gag in vitro. This

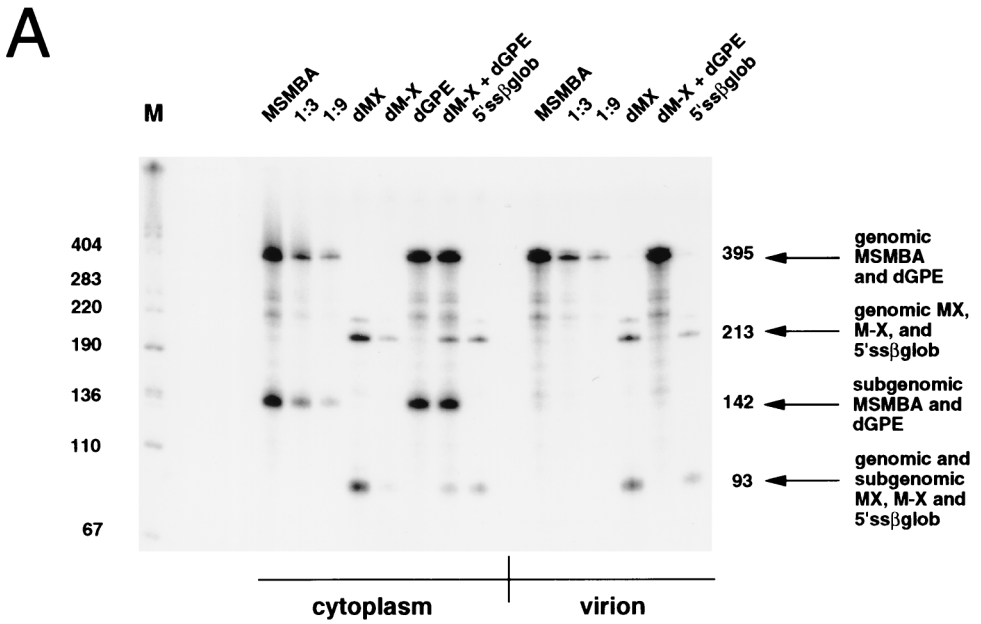

B Cytoplasm

	genomic RNA (Gag mRNA)	p24	p24/ RNA
MSMBA	1.00	1.00	1.00
dMX	0.62	1.54	2.48
dM-X	0.06	0.06	1.00
dGPE	1.02	N.A.	N.A.
dM-X + dGPE	0.21 1.02	0.38 N.A.	1.81 N.A.
5'ssβglob	0.21	0.40	1.90

C Virion

	p24	RNA/p24 genomic	RNA/p24 subgenomic
MSMBA	1.00	1.00	0.04
dMX	0.66	0.29	0.65
dM-X	0.02	N.D.	N.A.
dGPE	N.A.	N.A.	N.A.
dM-X + dGPE	0.43 N.A.	0.02 1.16	N.A. 0.05
5'ssβglob	0.21	0.08	0.23

FIG. 6. E is not required for translation in vivo. (A) RNase protection analysis of 293 cells transfected with the indicated plasmids in parallel. The probe used was generated from pGEM(600–1000) as described in the legends to Fig. 1 and 3. The analysis was performed on RNA isolated from equivalent amounts of cytoplasm or RNA from equivalent amounts of virions as determined by a p24 antigen capture assay (Coulter Cytometry) as described in the legend to Fig. 4. The MSMBA RNA analyzed was diluted 1:3 and 1:9 as indicated. M, molecular mass markers (in nucleotides). (B) The relative amounts of genomic RNA (Gag mRNA) within the cytoplasm of transfected cells are indicated. Values are normalized to the molar amount of genomic MSMBA RNA (1.00). The amounts of p24 within the cytoplasm of transfected cells are also indicated relative to the amount within the cells transfected with pMSMBA (1.00). N.A., not applicable. (C) The amounts of extracellular (virion) p24 and molar amounts of genomic and subgenomic RNA are indicated. Values are appropriately normalized to MSMBA p24 (1.00) or genomic MSMBA RNA (1.00). N.D., not done.

indicates that each of these hairpins is recognized by Gag. However, it is possible that SL1, SL3, and SL4 are not functionally identical in encapsidation.

Our results also show that SL1 contributes to specific encapsidation of genomic RNA and exclusion of spliced viral RNA. SL1 may interact with other elements within the viral intron, such as SL3 and SL4, to form a larger RNA tertiary structure that is recognized as E. This would be another consequence of a requirement for correct formation of a higher-order structure composed in part of SL1, SL3, and SL4. An alternative possibility, which is not mutually exclusive with the formation of a higher-order structure containing SL1, SL3, and SL4, is that splicing leads to the juxtaposition of downstream RNA sequences with the region containing SL1 which in turn leads to interference with the formation or function of SL1. Sequences adjacent to the encapsidation signal of Rous sarcoma virus, which is present on both genomic and subgenomic RNAs, may affect the overall secondary structure of E (2). It is important to note that SL1 is crucial in initiation of dimerization in vitro (3, 11, 12, 20, 24, 27, 29, 32). Thus, it is also possible that SL1 indirectly affects encapsidation by facilitating dimerization. Recently, others have observed that deletions of SL1 or mutations within the loop of SL1 reduce encapsidation (5, 28).

Examination of the primary sequences of diverse replication-competent HIV-1 strains indicates that there is some variation in both sequence and length of RNA sequences situated between individual hairpin structures in E. In examining the effect of switching the positions of hairpin structures, we also generated mutations in these spacer regions. These mutations by themselves had little effect on encapsidation efficiency. This observation, in conjunction with the variation exhibited in natural isolates, indicates that some of this region can be altered without affecting encapsidation. However, if the region encompassing SL1, SL3, and SL4 does assume a higher-order conformation, it is likely that further exploration of these spacer regions will result in the identification of nucleotides that are important for the proper overall conformation of the region.

We observed that SL1, SL2, and SL3 are not required for Gag mRNA translation; the reduction in expression of Gag observed for the mutant that lacks the region from the beginning of SL1 through the end of SL3 (pdM-X) can be completely attributed to the smaller amount of mRNA present within the cytoplasm. Furthermore, RNAs expressed from pdMX and p5′ssβglob may be translated more efficiently than wild-type RNA. This would be consistent with previous observations which indicated that deletion of E moderately increased translation efficiency of HIV-1 RNA in vitro (26) and that dimer formation of Rous sarcoma virus RNA inhibited translation in vitro (7).

Finally, although E does not appear to be important for translation of Gag mRNA in vivo, the region may be important for other steps in viral replication. The steady-state level of viral RNA expressed by viruses lacking this region was lower than the wild-type level, although the ratio of genomic RNA to subgenomic RNA was similar in each case. Others have observed that in addition to functioning in encapsidation, *cis* elements within the HIV-2 E negatively regulate Gag expression at the level of mRNA expression (13).

ACKNOWLEDGMENTS

We thank Katrin Talbot, Diccon Fiore, Mike Farrell, and Bob Cormier for technical assistance, Yung-Hui Lee and Michael D. Schwartz for critical reading of the manuscript, and Dan Loeb for helpful discussion.

M.S.M. was supported in part by a National Science Foundation (NSF) predoctoral fellowship and a Wisconsin Alumni Research Foundation (WARF) predoctoral fellowship. This work was supported by NIH grant RO1 AI34733.

REFERENCES

1. **Aldovini, A., and R. A. Young.** 1990. Mutations of RNA and protein sequences involved in human immunodeficiency virus type 1 packaging result in production of noninfectious virus. J. Virol. **64:**1920–1926.
2. **Aronoff, R., A. M. Hajjar, and M. L. Linial.** 1993. Avian retroviral RNA encapsidation: reexamination of functional 5′ RNA sequences and the role of nucleocapsid Cys-His motifs. J. Virol. **67:**178–188.
3. **Awang, G., and D. Sen.** 1993. Mode of dimerization of HIV-1 genomic RNA. Biochemistry **32:**11453–11457.
4. **Baudin, F., R. Marquet, C. Isel, J.-L. Darlix, B. Ehresmann, and C. Ehresmann.** 1993. Functional sites in the 5′ region of human immunodeficiency virus type 1 RNA form defined structural domains. J. Mol. Biol. **229:**382–397.
5. **Berkhout, B., and J. L. B. van Wamel.** 1996. Role of the DIS hairpin in replication of human immunodeficiency virus type 1. J. Virol. **70:**6723–6732.
6. **Berlioz, C., and J.-L. Darlix.** 1995. An internal ribosome entry mechanism promotes translation of murine leukemia virus *gag* polyprotein precursors. J. Virol. **69:**2214–2222.
7. **Bieth, E., C. Gabus, and J.-L. Darlix.** 1990. A study of the dimer formation of Rous sarcoma virus RNA and of its effect on viral protein synthesis in vitro. Nucleic Acids Res. **18:**119–127.
8. **Buchschacher, G. L., Jr., and A. T. Panganiban.** 1992. Human immunodeficiency virus vectors for inducible expression of foreign genes. J. Virol. **66:**2731–2739.
9. **Clavel, F., and J. M. Orenstein.** 1990. A mutant of human immunodeficiency virus with reduced RNA packaging and abnormal particle morphology. J. Virol. **64:**5230–5234.
10. **Clever, J., C. Sassetti, and T. G. Parslow.** 1995. RNA secondary structure and binding sites for *gag* gene products in the 5′ packaging signal of human immunodeficiency virus type 1. J. Virol. **69:**2101–2109.
11. **Clever, J. L., M. L. Wong, and T. G. Parslow.** 1996. Requirements for kissing-loop-mediated dimerization of human immunodeficiency virus RNA. J. Virol. **70:**5902–5908.
12. **Darlix, J.-L., C. Gabus, M. T. Nugeyre, F. Clavel, and F. Barre-Sinoussi.** 1990. *cis*-Elements and *trans*-acting factors involved in the RNA dimerization of the human immunodeficiency virus HIV-1. J. Mol. Biol. **216:**689–699.
13. **Garzino-Demo, A., R. C. Gallo, and S. K. Arya.** 1995. Human immunodeficiency virus type 2 (HIV-2): packaging signal and associated negative regulatory element. Hum. Gene Ther. **6:**177–184.
14. **Harrison, G. P., and A. M. L. Lever.** 1992. The human immunodeficiency virus type 1 packaging signal and major splice donor region have a conserved stable secondary structure. J. Virol. **66:**4144–4153.
15. **Hayashi, T., T. Shioda, Y. Iwakura, and H. Shibuta.** 1992. RNA packaging signal of human immunodeficiency virus type 1. Virology **188:**590–599.
16. **Jang, S. K., T. V. Pestova, C. U. Hellen, G. W. Witherell, and E. Wimmer.** 1990. Cap-independent translation of picornavirus RNAs: structure and function of the internal ribosome entry site. Enzyme **44:**292–309.
17. **Kaye, J. F., J. H. Richardson, and A. M. L. Lever.** 1995. *cis*-Acting sequences involved in human immunodeficiency virus type 1 RNA packaging. J. Virol. **69:**6588–6592.
18. **Kim, H.-J., K. Lee, and J. J. O'Rear.** 1994. A short sequence upstream of the 5′ major splice site is important for encapsidation of HIV-1 genomic RNA. Virology **198:**336–340.
19. **Konings, D. A. M., M. A. Nash, J. V. Maizel, and R. B. Arlinghaus.** 1992. Novel GACG-hairpin pair motif in the 5′ untranslated region of type C retroviruses related to murine leukemia virus. J. Virol. **66:**632–640.
20. **Laughrea, M., and L. Jette.** 1994. A 19-nucleotide sequence upstream of the 5′ major splice donor is part of the dimerization domain of human immunodeficiency virus type 1 genomic RNA. Biochemistry **33:**13464–13474.
21. **Lever, A., H. Göttlinger, W. Haseltine, and J. Sodroski.** 1989. Identification of a sequence required for efficient packaging of human immunodeficiency virus type 1 RNA into virions. J. Virol. **63:**4085–4087.
22. **Luban, J., and S. P. Goff.** 1994. Mutational analysis of *cis*-acting packaging signals in human immunodeficiency virus type 1 RNA. J. Virol. **68:**3784–3793.
23. **Maniatis, T., E. F. Fritsch, and J. Sambrook.** 1982. Molecular cloning: a laboratory manual. Cold Spring Harbor Laboratory, Cold Spring Harbor, N.Y.
24. **Marquet, R., J.-C. Paillart, E. Skripkin, C. Ehresmann, and B. Ehresmann.** 1994. Dimerization of human immunodeficiency virus type 1 RNA involves sequences located upstream of the splice donor site. Nucleic Acids Res. **22:**145–151.
25. **McBride, M. S., and A. T. Panganiban.** 1996. The human immunodeficiency virus type 1 encapsidation site is a multipartite RNA element composed of functional hairpin structures. J. Virol. **70:**2963–2973.
26. **Miele, G., A. Mouland, G. P. Harrison, É. Cohen, and A. M. L. Lever.** 1996. The human immunodeficiency virus type 1 5′ packaging signal structure affects translation but does not function as an internal ribosome entry site structure. J. Virol. **70:**944–951.
27. **Muriaux, D., P. M. Girard, B. Bonnet-Mathoniere, and J. Paoletti.** 1995. Dimerization of HIV-Lai RNA at low ionic strength. An autocomplementary sequence in the 5′ leader region is evidenced by an antisense oligonucleotide. J. Biol. Chem. **270:**8209–8216.
28. **Paillart, J.-C., L. Berthoux, M. Ottmann, J.-L. Darlix, R. Marquet, B. Ehresmann, and C. Ehresmann.** 1996. A dual role of the putative RNA dimerization initiation site of human immunodeficiency virus type 1 in genomic RNA packaging and proviral DNA synthesis. J. Virol. **70:**8348–8354.
29. **Paillart, J.-C., R. Marquet, E. Skripkin, B. Ehresmann, and C. Ehresmann.** 1994. Mutational analysis of the bipartite dimer linkage structure of human immunodeficiency virus type 1 genomic RNA. J. Biol. Chem. **269:**27486–27493.
30. **Parolin, C., T. Dorfman, G. Palú, H. Göttlinger, and J. Sodroski.** 1994. Analysis in human immunodeficiency virus type 1 vectors of *cis*-acting sequences that affect gene transfer into human lymphocytes. J. Virol. **68:**3888–3895.
31. **Richardson, J. H., L. A. Child, and A. M. L. Lever.** 1993. Packaging of human immunodeficiency virus type 1 RNA requires *cis*-acting sequences outside the 5′ leader region. J. Virol. **67:**3997–4005.
32. **Skripkin, E., J.-C. Paillart, R. Marquet, B. Ehresmann, and C. Ehresmann.** 1994. Identification of the primary site of the human immunodeficiency virus type 1 RNA dimerization *in vitro*. Proc. Natl. Acad. Sci. USA **91:**4945–4949.
33. **Tsukiyama-Kohara, K., N. Iizuka, M. Kohara, and A. Nomoto.** 1992. Internal ribosome entry site within hepatitis C virus RNA. J. Virol. **66:**1476–1483.
34. **Vagner, S., A. Waysbort, M. Marenda, M.-C. Gensac, F. Amalric, and A.-C. Prats.** 1995. Alternative translation initiation of the Moloney murine leukemia virus mRNA controlled by internal ribosome entry involving the p57/PTB splicing factor. J. Biol. Chem. **270:**20376–20383.
35. **Yang, S., and H. M. Temin.** 1994. A double hairpin structure is necessary for the efficient encapsidation of spleen necrosis virus retroviral RNA. EMBO J. **13:**713–726.